Modeling of a Hybrid Passive Damping System

Chul Hue Park*, Sang Jun Ahn, Hyun Chul Park
Department of Mechanical Engineering, Pohang University of Science and Technology (POSTECH), Pohang, KyungBuk, 790-784, Korea
Sungsoo Na
Department of Mechanical Engineering, Korea University, 1, 5-ga, Anam-dong, Sungbuk-gu, 136-701, Korea

The modeling of a hybrid passive damping system is presented for suppressing the multiple vibration modes of beams in this paper. This hybrid passive damping system consists of a constrained layer damping and a resonant shunt circuit. In a passive mechanical constrained layer damping, a viscoelastic layer, which is sandwiched between a host structure and a cover layer, is used to suppress vibration amplitudes in the high frequency range. A passive electrical damping is designed for targeting the vibration amplitude in the low frequency range. The governing equations of motion of the hybrid passive damping system are derived through the Hamilton's principle. The obtained mathematical model is validated experimentally. The theoretical and experimental techniques presented provide an invaluable tool in controlling the multiple vibration modes across a wide frequency band.

Key Words : Vibration Control, Shunt Circuit, Viscoelastic Material, Passive Damping

1. Introduction

Active damping has been shown to be an effective method due to its high power performance in controlling the unwanted vibration amplitudes of flexible structures (Bailey and Hubbard, 1985; Tzou and Tseng, 1991; Wang and Rogers, 1991; Yang and Lee, 1994, Chae and Park, 2002). A typical active damping treatment is a piezoelectric layer attached or embedded to the vibrating structure. With a proper controller design, the vibration energy dissipation can be enhanced by providing the electrical energy to the piezoelectric material. Hence, in order to obtain the high performance of the active damping system, it needs high-cost control especially at high frequency range (Park and Baz, 1999). Such problem can be avoided through the use of a passive damping treatment. The simple configuration of a mechanical passive damping treatment is to use a viscoelastic material (VEM), which is sandwiched between a host structure and a cover layer, called Passive Constrained Layer Damping (PCLD) treatment [Fig. 1a]. In a constrained viscoelastic layer the vibration energy of a host structure is dissipated through the shear deformation of a viscoelastic layer, which is bonded to a vibrating structure. Accordingly, the constrained damping layer is capable of dissipating higher vibrational energies and, in turn, achieving higher damping ratios, especially in the high frequency modes (Rao and Nakra, 1974).

Another form of passive damping treatments is the electrical passive shunt circuit (Fig. 1(b)). The shunt circuit consists of three electrical components : a capacitor C (PZT), an inductor and a resistor R, which is called a resonant shunt circuit (Hagood and Flotow, 1991, Moon et al., 2002). The two external terminals of the PZT, modeled

* Corresponding Author,
E-mail : drparkch@postech.ac.kr
TEL : +82-54-279-2962; **FAX** : +82-54-279-5899
Department of Mechanical Engineering, Pohang University of Science and Technology San31 Hyoja Dong, Pohang, KyungBuk, 790-784, Korea. (Manuscript **Received** December 8, 2003; **Revised** April 12, 2004)

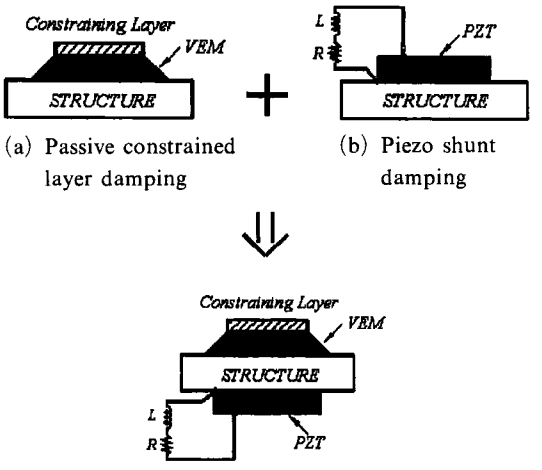

(a) Passive constrained layer damping (b) Piezo shunt damping

(c) Two passive damping treatments

Fig. 1 A hybrid passive damping system

as a capacitor, are connected to the series inductor and resistor shunt branch circuit. The piezoceramic element is used to convert mechanical energy of a vibrating structure into electrical energy by direct piezoelectric effect. This electric energy is dissipated as heat through the shunt resistor efficiently when the electric resonant frequency matches the mechanical resonant frequency. Therefore, a passive resonant shunt circuit has to be turned to suppress only a target mode as a mechanical vibration absorber.

In this paper, a hybrid passive damping system is used to control multi-mode vibration amplitudes of beams, which is combined the mechanical passive damping treatment with the electrical passive shunt circuit (Fig. 1(c)). Here, the passive constrained layer damping is used for suppressing the vibration amplitudes in the high frequency range. The shunt damper is augmented as an effective means to control the vibration amplitude in the low frequency range. Therefore, the hybrid system can be an excellent and practical means for controlling the vibration of massive structures with no need for large actuation voltages.

2. Equations of Motion of the Hybrid Passive System

A mathematical model is developed to describe

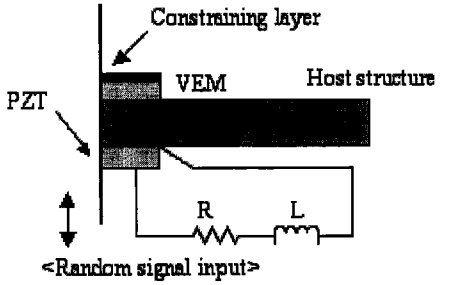

Fig. 2 Schematic drawing of the hybrid system

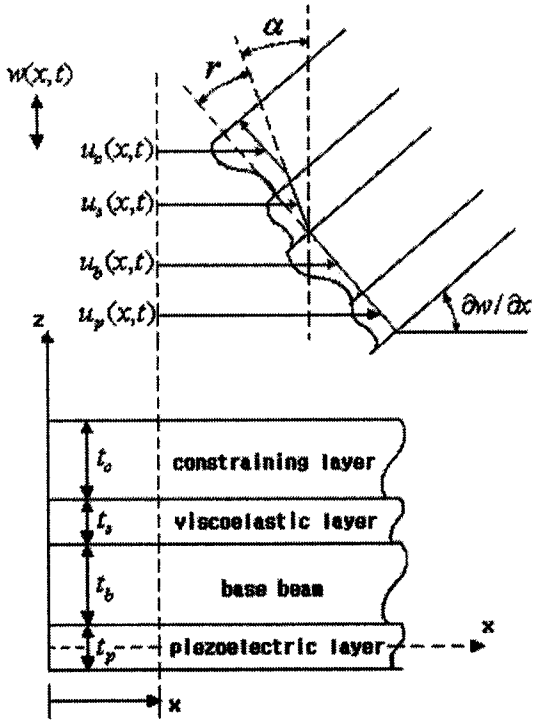

Fig. 3 Geometry and deformation of the hybrid system

the longitudinal, flexural, and shear strain behavior of the hybrid system in this section. The hybrid passive system consists of a host beam, a viscoelastic layer, a constraing layer, and a piezoelectric layer as shown in Fig. 2. A viscoelastic layer is sandwiched between a constraining layer and a host structure. A piezo layer is bonded to the lower surface of a beam and connected a series resonant shunt circuit. It is assumed that the shear strains in the beam layer, piezo layer, and cover layer are negligible and shear strains are con-

sidered only in the viscoelastic material. The transverse displacement, w, of all points on any cross-section of the laminated beam is considered to be equal. The damping layer is assumed to be linearly viscoelastic with their constitutive equations that are described using the shear complex modulus approach. The piezoelectric layer is assumed to be perfectly bonded and thin, so that electric displacement is constant through the thickness. Figure 3 shows the geometry and deformation of the hybrid passive system. The shear strain of the viscoelastic material can be defined as

$$r = \frac{\partial w}{\partial x} - \alpha \tag{1}$$

where w is the transverse displacement and α is the angle of rotation due to bending (Lam et al., 1997). The longitudinal displacements for the viscoelastic layer, cover layer, and piezoelectric layer can be described in terms of the longitudinal displacement of the beam layer as follows:

$$\begin{aligned} u_s &= u_b - \left(\frac{t_b+t_s}{2}\right)\frac{\partial w}{\partial x} + \frac{t_s}{2}r, \\ u_c &= u_b - d\frac{\partial w}{\partial x} + t_s r, \\ u_p &= u_b + \frac{t_b+t_p}{2}\frac{\partial w}{\partial x}. \end{aligned} \tag{2}$$

where t_b, t_s, t_c, t_p, is denoted the thicknesses of a beam layer, viscoelastic layer, constraining layer, and piezo layer, respectively. The subscript b refers to the host beam layer, s the viscoelastic layer, c the constraining layer, and p the piezo layer. The distance, d is

$$d = u_b + \left(\frac{t_b+t_p}{2}\right)\left(\frac{\partial w}{\partial x}\right) \tag{3}$$

The constitutive equation for a piezoelectric element depends on the mechanical stress, σ, and strain, ε, as well as the electric field, E, and the electric displacement, D. A common form of constitutive equations, especially, for a passive shunt damping is (IEEE, 1987)

$$\begin{bmatrix} \sigma \\ E \end{bmatrix} = \begin{bmatrix} E_s & -h \\ -h & \beta \end{bmatrix} \begin{bmatrix} \varepsilon \\ D \end{bmatrix} \tag{4}$$

where E_s is the elastic modulus at the constant displacement, h is the piezoelectric constant, and β is the dielectric constant.

The kinetic energy, T, expression for the laminated hybrid passive system is

$$T = T_b + T_s + T_c + T_p \tag{5}$$

where

$$\begin{aligned} T_b &= \frac{1}{2}\int_0^L \rho_b A_b \left[\left(\frac{\partial u_b}{\partial t}\right)^2 + \left(\frac{\partial w}{\partial t}\right)^2\right] dx, \\ T_p &= \frac{1}{2}\int_0^L \rho_p A_p \left[\left(\frac{\partial u_p}{\partial t}\right)^2 + \left(\frac{\partial w}{\partial t}\right)^2\right] \Delta H, \\ T_s &= \frac{1}{2}\int_0^L \rho_s A_s \left[\left(\frac{\partial u_s}{\partial t}\right)^2 + \left(\frac{\partial w}{\partial t}\right)^2\right] \Delta H dx, \\ T_c &= \frac{1}{2}\int_0^L \rho_c A_c \left[\left(\frac{\partial u_c}{\partial t}\right)^2 + \left(\frac{\partial w}{\partial t}\right)^2\right] \Delta H dx. \end{aligned}$$

The potential energy, V, of the hybrid system can be described as

$$V = V_b + V_c + V_p + V_s \tag{6}$$

where

$$\begin{aligned} V_b &= \frac{1}{2}\int_0^L E_b A_b \left[\left(\frac{\partial u_b}{\partial x}\right)^2 + E_b I_b \left(\frac{\partial^2 w}{\partial x^2}\right)^2\right] dx, \\ V_c &= \frac{1}{2}\int_0^L E_c A_c \left[\left(\frac{\partial u_c}{\partial x}\right)^2 + E_c I_c \left(\frac{\partial^2 w}{\partial x^2}\right)^2\right] \Delta H dx, \\ V_p &= \frac{1}{2}\int_0^L E_p A_p \left[\left(\frac{\partial u_p}{\partial x}\right)^2 + E_p I_p \left(\frac{\partial^2 w}{\partial x^2}\right)^2\right] \\ &\quad - 2A_p h_{31} D \left(\frac{\partial u_p}{\partial x}\right) - 2A_p h_{31} D z_p \left(\frac{\partial^2 w}{\partial x^2}\right) \\ &\quad + A_p \beta_{33}^s D^2 \Big] \Delta H dx \\ V_s &= \frac{1}{2}\int_0^L \left[E_s A_s \left(\frac{\partial u_s}{\partial x}\right)^2 + E_c I_c \left(\frac{\partial a}{\partial x^x}\right)^2 \right. \\ &\quad \left. + G_s A_s r^2\right] \Delta H dx, \end{aligned}$$

where A is the cross-sectional area and I the moment of inertia about the neutral axis for each layer and z_p is the distance from the neutral axis of the laminated beam to PZT. The material properties are defined by the density, ρ, and young's modulus, E. Here, D is the electric displacement of the PZT, h_{31} the piezoelectric constant, and β_{33}^s the dielectric constant. Heavisid e function, is ΔH, is $[H(x-x_1)-H(x-x_2)]$, which defines the length and position of the patch. The virtual work consists of three terms: the first one is for a work done by the piezo

resonant damper, the second is due to the external force, and the third is due to the inherent damping force.

$$\delta W=\int_0^L b V_{sh}(t)\,\delta D\Delta H dx+\int_0^L f(x,t)\,\delta w dx -\int_0^L C_b\frac{\partial w}{\partial t}Dw dx \tag{7}$$

The equations of motion and all the natural and geometric boundary conditions can be obtained by applying Hamilton's Principle,

$$\delta\int_1^2[T-V+W]dt=0. \tag{8}$$

where t_1 and t_2 are the end points in the time domain and δ is the virtual work parameter. Substituting the strain energy and kinetic energy into Hamilton's principle yields the following equations of motion.

$$\begin{aligned}&\rho_b A_b\left(\frac{\partial^2 w}{\partial t^2}\right)+(\rho_p A_p+\rho_s A_s+\rho_c A_c)\left(\frac{\partial^2 w}{\partial t^2}\right)\Delta H\\&-\left[\frac{1}{2}\rho_p A_p(t_b+t_p)-\frac{1}{2}\rho_s A_s(t_b+t_s)-\rho_c A_c d\right]\left(\frac{\partial^3 u_b}{\partial t^2\partial x}\right)\Delta H\\&-\left[\frac{1}{4}\rho_p A_p(t_b+t_p)^2+\frac{1}{4}\rho_s A_s(t_b+t_s)^2+\rho_c A_c d^2\right]\left(\frac{\partial^4 w}{\partial t^2\partial x^2}\right)\Delta H\\&+\left[\frac{1}{4}\rho_s A_s t_s(t_b+t_s)+\rho_c A_c d t_s\right]\left(\frac{\partial^3 r}{\partial t^2\partial x}\right)\Delta H+E_b I_b\left(\frac{\partial^4 w}{\partial t^4}\right)\\&+[E_p I_p+E_s I_s+E_c I_c+E_p I_p+\frac{1}{4}E_p A_p(t_b+t_p)^2\\&+\frac{1}{4}E_s A_s(t_b+t_c)^2+E_c A_c d^2]\left(\frac{\partial^4 w}{\partial x^4}\right)\Delta H\\&+\left[\frac{1}{2}E_p A_p(t_b+t_p)^2-\frac{1}{2}E_s A_s(t_b+t_s)^2+E_c A_c d\right]\left(\frac{\partial^3 u_b}{\partial x^3}\right)\Delta H\\&-\left[\frac{1}{4}E_s A_s t_s(t_b+t_s)+E_s I_s-E_c A_c d t_s\right]\left(\frac{\partial^3 r}{\partial x^3}\right)\Delta H=f(x,t)\end{aligned} \tag{9}$$

$$\begin{aligned}&\rho_b A_b\left(\frac{\partial^2 u_b}{\partial t^2}\right)+(\rho_p A_p+\rho_s A_s+\rho_c A_c)\left(\frac{\partial^2 u_b}{\partial t^2}\right)\Delta H\\&+\left[\frac{1}{2}\rho_p A_p(t_b+t_p)-\frac{1}{2}\rho_s A_s(t_b+t_s)-\rho_c A_c d\right]\left(\frac{\partial^3 w}{\partial t^2\partial x}\right)\Delta H\\&+\left[\frac{1}{2}\rho_s A_s t_s+\rho_c A_c t_s\right]\left(\frac{\partial^2 r}{\partial t^2}\right)\Delta H-E_b A_b\left(\frac{\partial^2 u_b}{\partial x^2}\right)\\&-(E_p A_p+E_s A_s+E_c A_c)\left(\frac{\partial^2 u_b}{\partial x^2}\right)\Delta H\\&-\left[\frac{1}{2}E_p A_p(t_b+t_p)-\frac{1}{2}E_s A_s(t_b+t_s)+E_c A_c d\right]\left(\frac{\partial^3 w}{\partial x^3}\right)\Delta H\\&-\left[\frac{1}{4}E_s A_s t_s+E_c A_c t_s\right]\left(\frac{\partial^2 r}{\partial x^2}\right)\Delta H=0\end{aligned} \tag{10}$$

$$\begin{aligned}&\left[\frac{1}{4}\rho_s A_s t_s^2+\rho_c A_c t_s^2\right]\left(\frac{\partial^2 r}{\partial t^2}\right)\Delta H\\&+\left[\frac{1}{2}\rho_s A_s t_s+\rho_c A_c t_s\right]\\&+\left[\frac{1}{4}E_s A_s t_s(t_b+t_s)+E_s I_s-E_c A_c d t_s\right]\left(\frac{\partial^3 w}{\partial x^3}\right)\Delta H\\&-\left[\frac{1}{2}E_s A_s t_s+E_c A_c t_s\right]\left(\frac{\partial^2 u_b}{\partial x^2}\right)\Delta H\\&-\left[\frac{1}{4}E_s A_s t_s^2+E_s I_s+E_c A_c t_s^2\right]\left(\frac{\partial^2 r}{\partial x^2}\right)+G_s A_s r=0\end{aligned} \tag{11}$$

Hamilton's principle also yields the following boundary conditions:

either $u_b=0$, or

$$\begin{aligned}&E_b A_b\left(\frac{\partial u_b}{\partial x}\right)+(E_p A_p+E_s A_s+E_c A_c)\left(\frac{\partial u_b}{\partial x}\right)\Delta H\\&+\left[\frac{1}{2}E_p A_p(t_b+t_p)-\frac{1}{2}E_s A_s(t_b+t_s)+E_c A_c d\right]\left(\frac{\partial^2 w}{\partial t^2}\right)\Delta H\\&+\left[\frac{1}{2}E_s A_s t_s+E_c A_c t_s\right]\left(\frac{\partial r}{\partial x}\right)\Delta H=-h_{31}t_p b D_3\Delta H\end{aligned} \tag{12}$$

either $w=0$, or

$$\begin{aligned}&E_b I_b\left(\frac{\partial^3 w}{\partial x^3}\right)+\left[E_p I_p+E_s I_s+E_c I_c+\frac{1}{4}E_p A_p(t_b+t_p)^2\right.\\&\left.+\frac{1}{4}E_s A_s(t_b+t_s)^2+E_c A_c d^2\right]\left(\frac{\partial^3 w}{\partial x^3}\right)\Delta H\\&+\left[\frac{1}{2}E_p A_p(t_b+t_s)-\frac{1}{2}E_s A_s(t_b+t_s)+E_c A_c d\right]\left(\frac{\partial^2 u_b}{\partial x^2}\right)\Delta H\\&-\left[\frac{1}{4}E_s A_s(t_b+t_s)t_s+E_s I_s-E_c A_c d t_s\right]\left(\frac{\partial^2 r}{\partial x^2}\right)\Delta H\\&=-h_{31}t_p b\left(\frac{t_b+t_p}{2}+z_p\right)D_3\Delta\mu\end{aligned} \tag{13}$$

either $\dfrac{\partial w}{\partial x}=0$, or

$$\begin{aligned}&E_b I_b\left(\frac{\partial^2 w}{\partial x^2}\right)+\left[E_p I_p+E_s I_s+E_c I_c+\frac{1}{4}E_p A_p(t_b+t_p)^2\right.\\&\left.+\frac{1}{4}E_s A_s(t_b+t_s)^2+E_c A_c d^2\right]\left(\frac{\partial^2 w}{\partial x^2}\right)\Delta H\\&+\left[\frac{1}{2}E_p A_p(t_b+t_s)-\frac{1}{2}E_s A_s(t_b+t_s)+E_c A_c d\right]\left(\frac{\partial u_b}{\partial x}\right)\Delta H\\&-\left[\frac{1}{4}E_s A_s(t_b+t_s)t_s+E_s I_s-E_c A_c d t_s\right]\left(\frac{\partial r}{\partial x}\right)\Delta H\\&=-h_{31}t_p b\left(\frac{t_b+t_p}{2}+z_p\right)D_3\Delta H\end{aligned} \tag{14}$$

either $r=0$, or

$$\left(\frac{1}{2}E_sA_st_s+E_cA_ct_s\right]\left(\frac{\partial u_b}{\partial x}\right)\Delta H$$
$$-\left[E_sA_s+\frac{1}{4}E_sA_s(t_b+t_s)\,t_s-E_cA_cdt_s\right]\left(\frac{\partial^2 w}{\partial x^2}\right)\Delta H \quad (15)$$
$$+\left[\frac{1}{4}E_sA_st_s^2+E_sI_s+E_cA_ct_s^2\right]\left(\frac{\partial r}{\partial x}\right)\Delta H=0$$

where the function, $\Delta\mu$, is $[\mu(x-x_1)-\mu(x-x_2)]$, which represents two concentrated sources at x_1 and x_2, respectively. The assumed mode method is used to discretize the equations of motion [Eqs. (9)-(11)] into a set of ordinary differential equation. The shape functions for the series expansions are used to expand the transverse, longitudinal displacement, and shear strain functions, w, u_b, r, respectively (Meirovitch, 1967).

$$w(x,t)=\sum_{n=1}^{n}W_n(x)\,\phi_n(t),$$
$$u_b(x,t)=\sum_{n=1}^{n}U_n(x)\,\theta_n(t), \quad (16)$$
$$r(x,t)=\sum_{n=1}^{n}\Upsilon_n(x)\,\Psi_n(t)$$

The displacement functions, $W_n(x)$, $U_n(x)$, $\Upsilon_n(x)$ are sets of admissible functions which are chosen for each generalized modal coordinate, $\phi_n(t)$, $\theta_n(t)$, $\Psi_n(t)$ respectively. Applying mode shape functions to the equation of motion, Eqs. (9)-(11) results in the following discretized differential equations of the hybrid passive system.

$$M\ddot{W}(t)+C\dot{W}(t)+KW(t)=f_{ext}+f_{piezo} \quad (17)$$

where $f_{ext}=\left[\int_0^L\phi_nf(x,t)\,dx,0,0\right]^{-T}$ and $f_{piezo}=[f_{p1}\ f_{p2}\ 0]^T\ V_{sh}(t)$ with

$$f_{p1}=-bd_{31}E_pz_p\int_0^L W_i[\delta'(x-x_1)-\delta'(x-x_2)]\,dx,$$
$$f_{p2}=-bd_{31}E_pz_p\int_0^L U_i[\delta(x-x_1)-\delta(x-x_2)]\,dx.$$

3. Shunt Voltage and Shunt Parameters of the Hybrid System

The charge generated by the PZT patch due to the structural vibration of the cantilever beam can be sought from the electric field displacement, $[D]$ as follows:

$$Q(t)=\int_A D\,dA \quad \text{with}$$
$$[D]=[d]^T\{T\}+[\varepsilon]^T\{E\} \quad (18)$$

where $[d]$, $\{T\}$, $[\varepsilon]$ and $\{E\}$ represent the piezoelectric strain constant, stress, dielectric permittivity, applied electric field, respectively. Substituting the mode shape function into Eq. (18), the output of piezo sensor can be derived as follow:

$$Q_i(t)=(C_1D_{1n}+C_2D_{2n}+C_p^T\,V_{sh})$$
$$[H(x-x_1)-H(x-x_2)] \quad (19)$$

where $C_1=d_{31}E_pb_p$, $D_{1n}=\sum_{n=1}^{n}\int_0^L\frac{\partial U_n}{\partial x}\Delta H dx$,

$$C_2=-d_{31}E_pb_p((t_b+t_p)/2+z_p),$$
$$D_{2n}=\sum_{n=1}^{n}\int_0^L\frac{\partial^2 W_n}{\partial x^2}\Delta H dx. \quad (20)$$

By differentiating the induced charge of the piezoelectric sensor with respect to time, the current across PZT electrodes can be obtained.

$$I_i(t)=\frac{dQ_i}{dt}=[C_1D_{1n}\,s\theta(s)+C_2D_{2n}\,s\phi(s)$$
$$+C_p^T s\,V_{sh}] \quad (21)$$

From the sensor current, the shunt voltage can be sought as follows:

$$V_{sh}=-\frac{Ls+R}{LC_p^Ts^2+RC_p^Ts+1}\begin{bmatrix}C_2D_{2n}\\C_1D_{1n}\\0\end{bmatrix}^T\begin{bmatrix}\dot{\phi}(t)\\\dot{\theta}(t)\\\dot{\Psi}(t)\end{bmatrix} \quad (22)$$

Here, the inherent capacitance of the PZT should be determined by using the below equation.

$$C_p^T=\frac{K_3^T\times\varepsilon_0\times A_p}{t_p} \quad (23)$$

where C_p^T is the capacitance of the PZT at constant stress, K_3^T is the relative dielectric constant at 1KHz, and the constant ε_0 is 8.85×10^{-12}F/m, A_p is the surface area of PZT. The product of $K_3^T\,\varepsilon_0$ is called the permittivity of the dielectric

denoted ε. The required inductor and shunt resistor values in Eq. (22) are calculated from the following equation.

$$L=\frac{1}{\omega_e^2 C_p^S},\quad R=\frac{\gamma_{opt}}{C_p^S\omega_n^E} \tag{24}$$

where ω_e is the electrical resonant frequency. The PZT capacitance at constant strain, C_p^S, is obtained from the following equation which is dependent upon the electromechanical coupling coefficient, k_{31} provided by the manufacturer.

$$C_p^S=C_p^T(1-k_{31}^2) \tag{25}$$

The tuning parameter, γ_{opt}, is calculated from the generalized electromechanical coupling constant (Hagood's, 1991) :

$$\gamma_{opt}=1.414\frac{K_{31}}{1+K_{31}^2}\quad \text{where}$$
$$K_{31}^2=\{(\omega_n^D)^2-(\omega_n^E)^2\}/(\omega_n^E)^2 \tag{26}$$

Here ω_n^D and ω_n^E are the natural frequencies of the structural mode of interest with an open circuit and a short circuit piezoelectric, respectively.

4. Experimental Implementation

Experiments were performed to examine the performance behaviors of the hybrid system. A PZT 5H (Fuji ceramics, 50×20mm) was bonded to the lower surface of an aluminum beam (220×20mm) by using epoxy adhesive. This edge of the piezoceramic was 0.1cm away from a fixed end of the beam. This fixed end was clamped horizontally in a rigid support fixture that was excited by an electro-magnetic shaker (TIRA, Vib5200). The internal function generator of the spectrum analyzer (HP 3566A) is used to generate a random excitation signal from 1Hz to 500Hz. A gab sensor (Kaman, KD2300-6C) was located at the free end of the beam to measure the system output responses. A sandwiched viscoelastic core (SOUNDCOAT, 50×20mm) is used as the damping material. An aluminum cover layer (50×20×0.05mm) is used as a constraining layer. Tables 1 and 2 show the main physical and geometrical parameters of the aluminum, DYAD and PZT 5H. An active filter (Horowitz and Hill, 1989) is used as a synthetic inductor in the shunt branch circuit as shown in Fig. 4. The advantages of this inductor are due to its convenience, lightweight, its ability to generate various inductances. R_4 is ordinarily a capacitor, with the other impedances being replaced by resistors, creating an inductor $L=R^*C$, where $R^*=R_1R_3R_5/R_2$. By changing the variable resistor R_2, various inductance values could be obtained. The resistance value 10,000 Ω for R_1, R_3, R_5 and the capacitance $10nF$ for R_4 are used for this analysis.

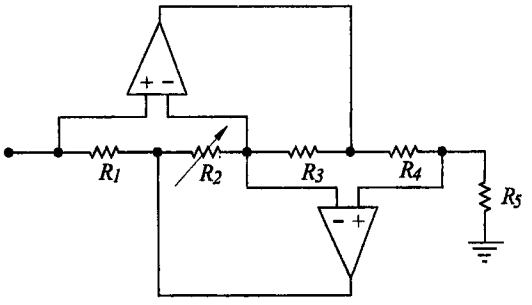

Fig. 4 Circuit diagram of a synthetic inductor.

Table 1 Physical and geometrical properties of the beam, viscoelastic and PZT layer.

.	Young's modulus (Pa)	Density (kg/m³)	Poisson's Ratio (ν)	Thickness (mm)
Al beam	7.0E10	2700	0.33	1.5
DYAD-606	*	1104	0.49	0.508
PZT	5.9E10	7400	0.3	0.5

* Depending on temperature and frequency

Table 2 Main piezoelectric parameters of the PZT-5H.

d_{31} (m/V)	g_{31} (Vm/N)	k_{31} Coupling Coef.	K_{31} Dielectric	Dissipation Factor	Curie Temp. (°C)
-260E-12	-8.7 E-3	0.36	3100	1.8%	190

5. Results and Discussions

The performances of the hybrid passive system are discussed as considering a series resonant shunt circuit for suppressing the first frequency mode and a PCLD patch for high frequency vibration amplitudes. As shown in Fig. 5, the electrical passive damping is tested experimentally and theoretically to reduce the vibration amplitudes of the first bending mode of the hybrid system. It is evident that decreasing the resistance results in improving the vibration attenuation characteristics of the first bending mode. When the resistance is decreased below the optimal resistance [when the peak becomes a flat plateau], the two peaks rise up, exactly as it does in the case of a mechanical absorber. The electrical passive damping is found to produce about 17dB reduction from the peak vibration amplitude of the open circuit. The optimum resistance value was chosen from the Eq (24) at first and then was a little bit adjusted for the optimum by a trial-and-error method. Because the gyrator circuit is not a pure inductor, it creates a resistive component which is not desirable for designing the optimal resistance in the shunt branch circuit.

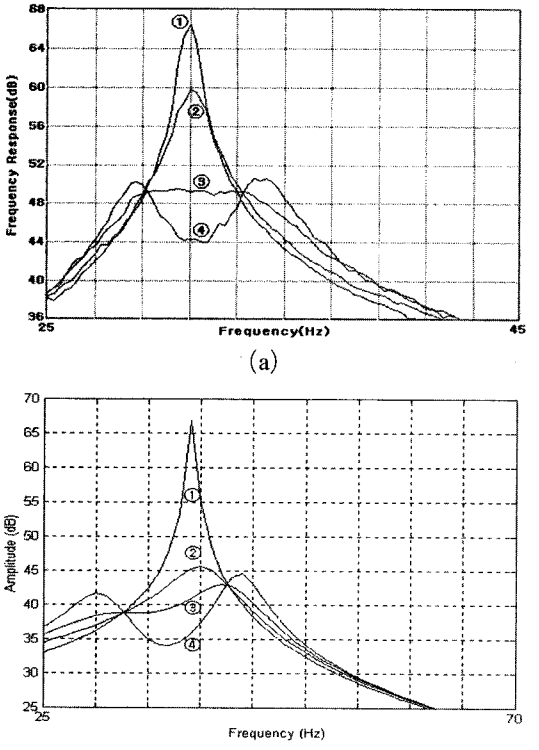

Fig. 5 Transfer responses of the hybrid system for the first mode: (a) Experiment (b) Theory. [①: Open ②: 40,000Ω ③: 18,230Ω ④: 8,140Ω].

The performances are obtained from the experimental testing done for two cases: an unconstrained layer damping (without a cover layer) and a constrained layer damping (with a cover layer). As shown in Table 3, the magnitudes of the first, second, and third mode are reduced by 0.6dB (6.7%), 1.4dB (15%) and 1.7dB (17%), respectively, from the peak amplitude of a plain beam for the case of unconstrained layer damping. The constrained layer damping suppresses the first mode by 2.1dB (21%), the second mode by 5.1dB (44%) and the third mode by 9.2dB (65%). It can be concluded that the constrained layer damping is superior to the unconstrained layer damping in view of vibration reduction performance. Such superiority stems from the fact that the constrained layer damping layer experiences shear strain which are much larger than that encountered in the unconstrained layer damping. This feature is displayed clearly in Fig. 6.

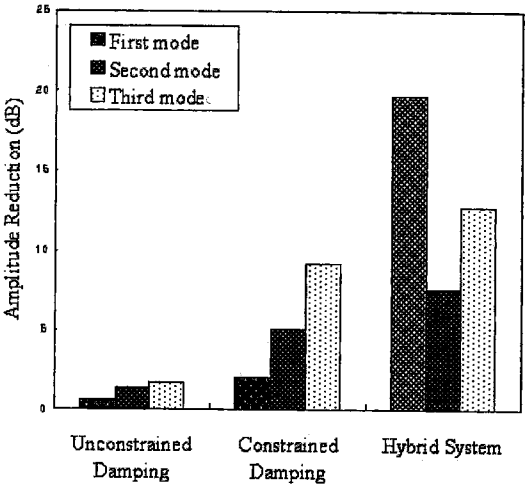

Fig. 6 Comparison between amplitude reductions of the unconstrained, constrained layer damping, and hybrid system

Table 3 Vibration amplitude attenuations of unconstrained, constrained, and hybrid system.

	1st mode (Attenuation)	2nd mode (Attenuation)	3rd mode (Attenuation)
Unconstrained	0.6dB (6.7%)	1.4dB (15%)	1.7dB (17%)
Constrained	2.1dB (21%)	5.1dB (44%)	9.2dB (65%)
Hybrid system	19.7dB (89%)	7.6dB (58%)	12.7dB (77%)

Finally, two passive systems, the resonant shunt circuit and the constrained layer damping, were operated simultaneously to suppress the multiple modes over the broad frequency range as shown in Fig. 7. The vibration amplitudes are measured of 19.7dB (89.6%) reduction for the first mode, 7.6dB (58.4%) for the second mode, and 12.7dB (76.9 %) for the third mode as shown in Fig. 6. Also, the theoretical natural frequencies of the plain beam, unconstrained layer damping, constrained layer damping, and hybrid system are compared with experimental measurements for the first, second, and third modal frequencies as shown in Fig. 8. The results show a good agreement in the natural frequencies evaluated by two methods. The discrepancy is about 2-3% for the plain beam and unconstrained layer damping and

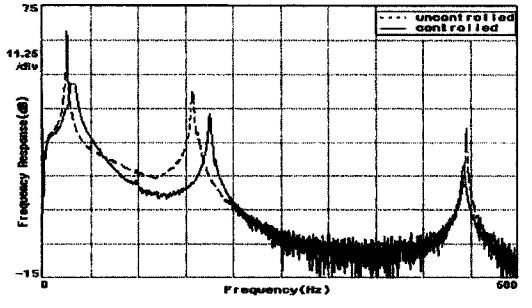

(a)

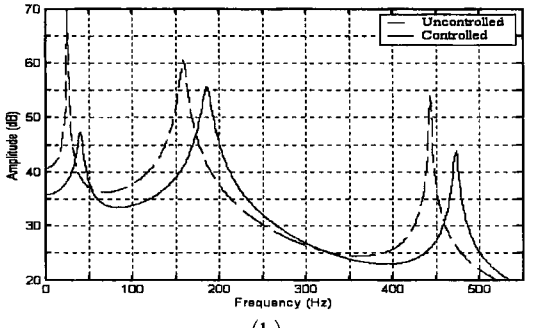

(b)

Fig. 7 Transfer responses of the hybrid system : (a) Experiment (b) Theory.

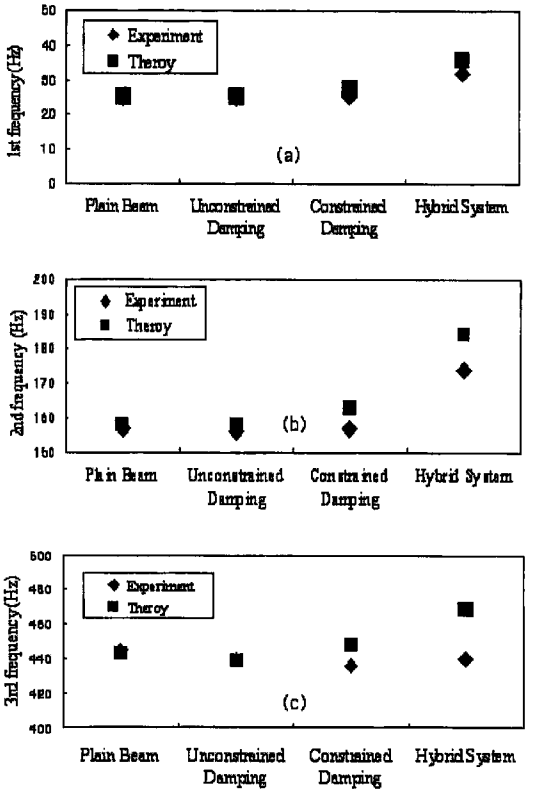

Fig. 8 Comparison between theoretical and experimental natural frequencies of the plain beam, unconstrained, constrained layer damping, and hybrid system

5-7% for the constrained layer damping and hybrid system.

6. Conclusions

Hybrid system is devised by combining the mechanical passive damping treatment with the electrical passive damping. The mechanical passive treatment provides a fail-safe damping and improves the stability of the system. The resonant shunt circuit is augmented for suppressing a vibration mode in the low frequency range. The

equations of motion are derived using Hamilton's principle. Assumed modes are used to discretize these equations. The shunt voltage was formulated from the charge generated by the piezoceramic due to the direct piezoelectric effect. The derived mathematical model was validated experimentally. The results showed a good agreement in between theory and experiment.

Acknowledgments

This work was supported by Korea Research Foundation Grant (KRF-2002-041-D00028).

References

Bailey, T. and Hubbard, J., 1985, "Distributed Piezoelectric Polymer Active Vibration Control of a Cantilever Beam," *Journal of Guidance, Control, and Dynamics*, Vol. 8, pp. 605~610.

Chae, J. and Park, T., 2002, "H_∞ Controller Design of Flexible Space Structure with the Uncertainty of Damping Ratio," *Transactions of KSME*, Vol. 26, No. 4 pp. 602~608 in Korea.

Hagood, N. and von Flotow, A., 1991, "Damping of Structural Vibrations with Piezoelectric Materials and Passive Electrical Networks," *Journal of Sound and Vibration*, Vol. 146(2), pp. 243~268.

IEEE, 1987, *IEEE standard on piezoelectricity* (IEEE Std 176-1987), Piscataway, NJ.

Lam, M., Inman, D. and Saunders, W., 1997, "Vibration Control Through Passive Constrained Layer Damping and Active Control," *Journal of Intelligent Material Systems and Structures*, Vol. 8, pp. 663~667.

Meirovitch, L., 1967, *Analytical methods in vibrations*, London : The Macmillan Company.

Horowitz, P. and Hill, W., 1989, *The art of electronics*, Cambridge : Cambridge University Press.

Moon, S., Yun, C. and Kim, S., 2002, "Passive Suppression of Nonlinear Panel Flutter Using Piezoelectric Materials with Resonant Circuit, "*KSME International Journal*, Vol. 16, No. 1, pp. 1~12 in Korea.

Park. C. and Baz A., 1999, "Vibration Damping and Control Using Active Constrained Layer Damping : A Survey," *The Shock and Vibration Digest*, Vol. 31, pp. 355~364.

Rao, Y. V. K. S. and Nakra, B. C., 1974, "Vibrations of Unsymmetric Sandwich Beams and Plates with Viscoelastic cores," *Journal of Sound and Vibration*, Vol. 34, pp. 309~326.

Tzou, H. and Tseng, C., 1991, "Distributed Modal Identification and Vibration Control of Continua : Piezoelectric Finite Element Formulation and Analysis," *Journal of Dynamic Systems, Measurement, and Control*, Vol. 113, pp. 500~505.

Wang, B. T. and Rogers, C. A. 1991, "Laminate Plate Theory for Spatially Distributed Induced Strain Actuators," *Journal of Composite Materials*, Vol. 25, pp. 433~452.

Yang, S. and Lee, Y., 1994, "Interaction of Structure Vibration and Piezoelectric Actuation," Smart Materials and Structures, Vol. 3, pp. 494~499.